

A Density Functional Theory Study on Pelargonidin

Laura Estévez and Ricardo A. Mosquera*

Departamento de Química Física, Facultad de Química, Universidade de Vigo, Lagoas-Marcosende
s/n 36310-Vigo Galicia, Spain

Received: June 25, 2007; In Final Form: July 27, 2007

A complete conformational analysis on the isolated and polarizable continuum model (PCM) modeled aqueous solution cation, quinonoidal, and anion forms of pelargonidin, comprising the diverse tautomers of the latter forms, was carried out at the B3LYP/6-31++G(d,p) level. The results indicate that the most stable conformer of cationic and quinonoidal forms of pelargonidin are completely planar in the gas phase, whereas that of the anionic form is not planar. In contrast, PCM calculations show that the plane of the **B** ring is slightly rotated with regard to the **AC** bicycle in the most stable conformer of the cation and quinonoidal form. The most stable conformers of the cation, both in gas phase and aqueous solution, display anti and syn orientations for, respectively, C2–C3–O–H and C6–C5–O–H dihedral angles, whereas syn and anti orientation of hydroxyls at 7 and 4' positions are nearly isoenergetic. The most stable tautomer of quinonoidal pelargonidin is obtained by deprotonating hydroxyl at C5 in gas phase but at C7 according to PCM. Also, the most stable tautomer of the anion is different in gas phase (hydrogens are abstracted from hydroxyls at C5 and C4') and PCM simulation (C3 and C5). Tautomeric equilibria affect substantially the geometries of the **AC–B** backbone providing bond length variations that basically agree with the predictions of the resonance model. Most of the conformers obtained display an intramolecular hydrogen bond between O3 and H6'. Nevertheless, this interaction is not present in the most stable anions. Ionization potentials and O–H bond dissociation energies computed for the most stable conformers of cation, quinonoidal, and anion forms are consistent with an important antioxidant activity.

Introduction

Anthocyanins (glycosylated polyhydroxy derivatives of 2-phenylbenzopyrylium salts) are defined as natural, water-soluble, nontoxic pigments responsible for some colors of fruits, vegetables, flowers, and other plant tissues.¹ They are commonly found in red wine and fruit juices and have been shown to have properties beneficial to human health, including antioxidant² and antitumor³ activity. As no harmful effects have been established, anthocyanins have considerable potential as food additives, and the use of these pigments as natural colorants to replace synthetic dyes has been proposed.^{4–9} However, because of their instability toward some chemical and physical parameters such pH and light, their use in the food industry has not been extensively developed.

It is known that anthocyanins may exist in a variety of protonated, deprotonated, hydrated, and isomeric forms, whose relative proportion is strongly dependent on pH. The red flavylium cation is dominant at very acidic pH (pH 1–3). In aqueous media, as the pH is raised to 4–5, hydration reactions generate the colorless carbinol pseudobase, which can further undergo ring opening to the light-yellow chalcones, most rapidly at pH 2.5–5 at increased temperatures. The flavylium cation can alternatively be transformed to quinonoidal bases through proton-transfer reactions and at values between 6 and 7 can be further converted to the blue-purple quinonoid anions.^{10,11}

Because of their antioxidant properties, anthocyanins are considered as a group of polyphenolic antioxidants. As for other polyphenolics, their antioxidant ability has been related to low

O–H bond dissociation enthalpy (BDE) and relatively high ionization potential (IP).^{12–15} The first feature facilitates the H-abstraction reaction between the antioxidant and the radical. Relatively high IP decreases the electron-transfer rate between the antioxidant and the oxygen and thus reduces pro-oxidative potency of the oxidant. Nevertheless, it has to be noticed that relatively low IP can be also related to enhanced antioxidant activity through a mechanism involving electron transfer and proton transfer steps.

Anthocyanins generally occur as glycosides, whose bioactivity is attributed to the aglycon but not to the sugar or other binding species.¹⁶ Thus, the computational study of these compounds can be concentrated on that of the aglycons, which are known as anthocyanidins.

Some theoretical studies on the stable structures of anthocyanidins have already been reported. Nevertheless, practically all of them employ exclusively semiempirical,^{17–20} noncorrelated Hartree–Fock²¹ levels, or molecular mechanics and simulation methods.²² One study²³ performed post-Hartree–Fock calculations, employing both MP2 and density functional theory (DFT), but was limited to the flavylium cation and its monohydroxylated derivatives. Two recent papers^{24,25} perform a detailed conformational study of the cationic form of diverse anthocyanidins using the B3LYP DFT functional with 6-31G(d) and D95 basis sets. To the best of our knowledge, there has been no previous DFT study on the whole set of prototropic forms of anthocyanidins.

Furthermore, theoretical results obtained on isolated molecules can be compared to experiments only in a few cases, since most of the experiments are performed in liquid solutions. For this reason, numerous models have been developed for taking into

* To whom correspondence should be addressed. E-mail: mosquera@uvigo.es.

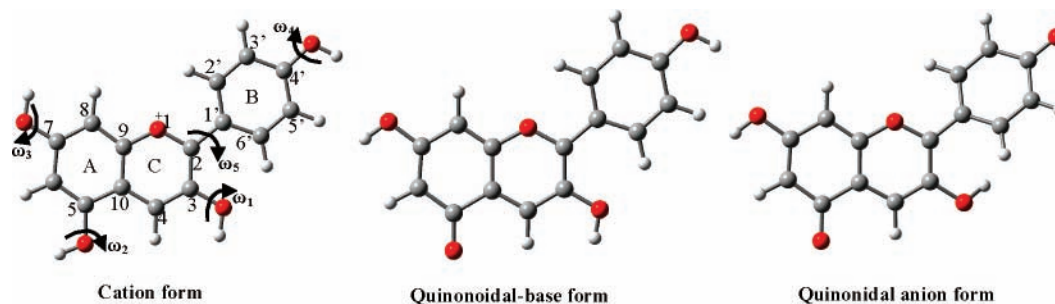


Figure 1. Most stable rotamers of cationic, quinonoidal, and anionic forms of pelargonidin showing the labeling scheme for the three rings (A, B, C), atom numbering, and main dihedral angles (ω_1 – ω_5).

account solute–solvent interactions in quantum chemical calculations. Continuum solvent models are particularly attractive since they can be both reliable and very effective. The polarizable continuum model (PCM), first proposed by Miertu et al.,²⁶ has proven to be a reliable tool for the description of electrostatic solute–solvent interactions.²⁷

Pelargonidin (Figure 1) forms with delphinidin and cyanidin the three anthocyanidins known as the principal and basic skeletons of flowers color pigments. In conformational terms, it can be considered as the basic anthocyanidin because it has the smallest number of hydroxyl groups. This makes it the most available anthocyanidin for performing a detailed conformational study that considers all the possible rotamers, tautomers, and forms in the molecule. Even assuming a preferred orientation for 3-OH, there are 48 different rotamers in pelargonidin. The number of different rotamers susceptible for yielding different conformers exceeds 300 rotamers in delphinidin. This reflects the high computational cost of complete conformational analysis. In consequence, reliable structural trends for these compounds would be very convenient for reducing the conformational search in polysubstituted anthocyanidins. Therefore, the present study investigates the structural stabilities of pelargonidin using DFT calculations to describe its main conformational trends. We examine the structural characteristics in the solvent-free and water-solvent cationic, quinonoidal, and anionic forms of pelargonidin. Finally, taking into account the radical-scavenging capacity of anthocyanins, we also compute IPs and O–H BDEs for the diverse acid/base forms of pelargonidin that successfully compare with those of other natural and commercial antioxidants.

Computational Details

The geometries of pelargonidin in its different forms (flavylium cation, quinoidal-base, and anionic forms) were fully optimized with the B3LYP²⁸ hybrid density functional theory (DFT) by using the 6-31++G(d,p) basis set as implemented in Gaussian03 package.²⁹ The optimized conformations were confirmed as true minima by vibrational analysis at the same level. Solvation free energies were computed using the polarizable continuum model (PCM)³⁰ from the geometries optimized with this method. Vibrational frequency analysis was also carried out to characterize the stationary states obtained with PCM optimizations.

Unrestricted UB3LYP/6-31++G(d,p) complete optimizations were carried out for the radical species obtained as a result of the ionization or O–H bond cleavage experienced by the most stable conformer of each of the pelargonidin forms. These calculations were employed to obtain ionization potentials, PI, and O–H bond dissociation enthalpies, BDE, for cationic, quinonoidal, and anionic forms of pelargonidin (Figure 1). PIs

and BDEs were obtained including zero point vibrational energies (ZPVE) and other thermal corrections to the enthalpy (TCE) of final and initial states.

Conformations are named by acronyms made by a capital letter indicating the concrete acid/base form of pelargonidin considered (C = cation, Q = quinonoidal, A = anion) and four lower case letters indicating approximated values of the main dihedral angles defining the orientation of the hydroxyl groups. They are ω_1 (C2–C3–O–H), ω_2 (C5–C6–O–H), ω_3 (C6–C7–O–H), and ω_4 (C3'–C4'–O–H); *s* denotes nearly syn-periplanar and *a* denotes nearly anti-periplanar. Another important dihedral angle is ω_5 (O1–C2–C1'–C2') that defines the coplanarity of AC and B systems (Figure 1). Bearing in mind the different number of OH groups presented by C, Q, and A forms and the presence of multiple tautomers in Q and A, the position of symbol *x* indicates which hydroxyl has been deprotonated.

Results and Discussion

A detailed conformational analysis was performed for the three forms of pelargonidin (C, Q and A) both in gas and in the PCM modeled solvated phase. The results are presented below in separated epigraphs for cationic, quinonoidal, and anionic forms. In all cases, the results are first presented for the isolated molecules in gas phase and then for the PCM modelization of the aqueous solution.

Cationic Form. We have optimized eight different initial conformations resulting from considering *a* and *s* arrangements for ω_2 , ω_3 , and ω_4 dihedral angles. Taking into account previous studies²⁵ and expected high repulsions between H6' and H3 if ω_1 is in *s* arrangement, this dihedral angle was considered in disposition *a* in all the initial conformations, although we have checked the validity of this assumption (see below). *Casaa* has been found as the most stable conformer of this form in gas phase. Internal rotation around ω_1 (Figure 2a) was performed for this conformer, and we have observed a rotational barrier of 12 kJ mol⁻¹ for the interconversion to a shallow minimum (*Cssaa*) whose relative energy is 8 kJ mol⁻¹ above *Casaa*, confirming previous results and expectations on the basis of qualitative estimations of steric repulsions.

It is noticeable that restricted optimizations with *C_s* symmetry from initial conformations with ω_2 anti-periplanar (*Caa--*) give rise always to transition states with one imaginary frequency. Their relative energies (Table 1) are between 19 and 20 kJ mol⁻¹ (after ZPVE corrections) over the corresponding *s* structure. The internal rotation of ω_2 shows that the true *Caa--* minima display ω_2 values around 170° (Figure 2b). The energy difference between the true *Caa--* local minimum and the planar transition state is negligible (0.02 kJ mol⁻¹).

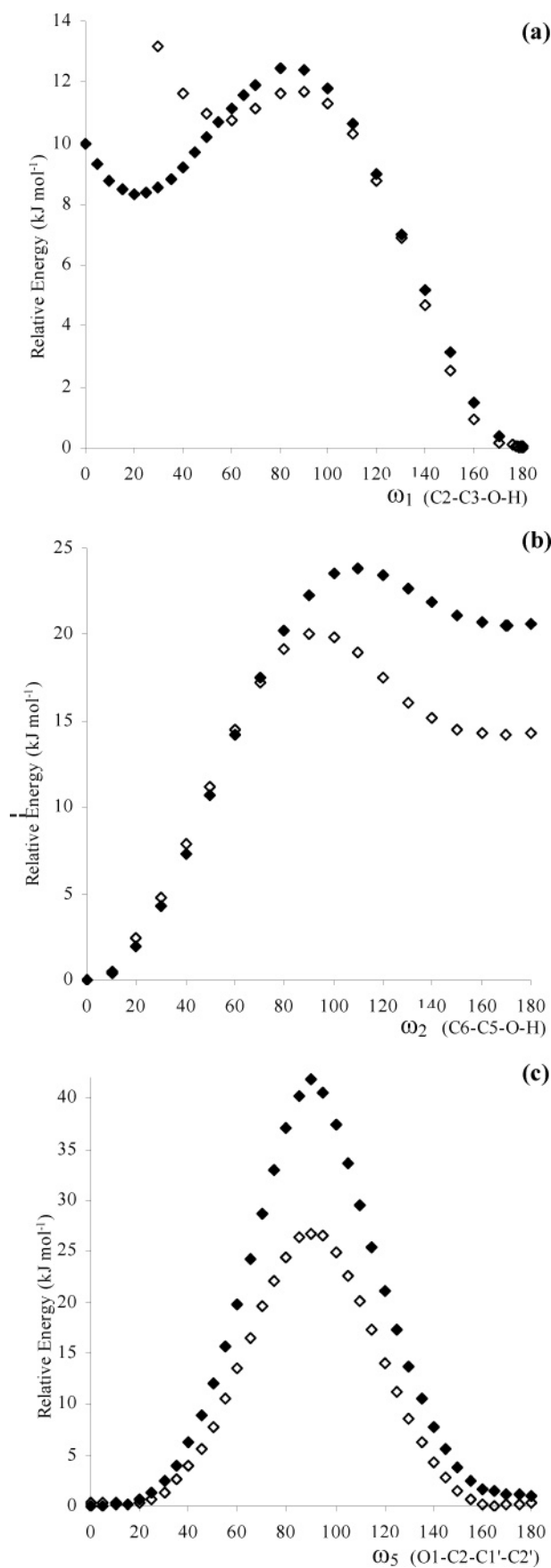


Figure 2. Energy profiles for the internal rotation around ω_1 (C2–C3–O3–H3) (a), ω_2 (C6–C5–O5–H5) (b), and ω_5 (O1–C2–C1'–C2') (c) for the most stable cation (*Casaa*) of pelargonidin. Bold face symbols refer to isolated molecule and open face symbols refer to PCM calculations.

TABLE 1: B3LYP/6-31++G(d,p) Relative Energies (in kJ mol⁻¹) for Isolated Pelargonidin Rotamers

rotamer	IFN ^a	ΔE^b	rotamer	IFN ^a	ΔE^b	rotamer	IFN ^a	ΔE^b
<i>Casaa</i>	0	0.0	<i>Qaxsa</i>	0	0.0	<i>Asxxx</i>	0	0.0
<i>Casas</i>	0	1.0	<i>Qaxss^{c,d}</i>	0	0.1	<i>Aaxsx</i>	0	0.5
<i>Cassa</i>	0	1.5	<i>Qxsa</i>	0	6.0	<i>Asxax</i>	0	3.8
<i>Casss</i>	0	2.2	<i>Qasxs</i>	0	6.1	<i>Aaxax</i>	0	4.3
<i>Caasa</i>	1	19.8	<i>Qasxa</i>	0	6.1	<i>Assxx</i>	0	6.0
<i>Caass</i>	1	20.3	<i>Qxasa</i>	0	6.8	<i>Axaax</i>	0	6.4
<i>Caaaa</i>	1	21.9	<i>Qaxaa</i>	0	7.0	<i>Axasx</i>	0	7.9
<i>Caaas</i>	1	22.7	<i>Qxaaa</i>	0	7.0	<i>Axxsa</i>	0	9.4
			<i>Qaxas^{c,e}</i>	0	7.3	<i>Axxss</i>	0	10.8
			<i>Qxsas</i>	0	8.3	<i>Aasxx</i>	0	11.5
			<i>Qxass</i>	0	8.7	<i>Axsxa</i>	0	12.0
			<i>Qxaas</i>	0	9.2	<i>Axaxa</i>	0	12.7
			<i>Qxssa</i>	0	9.2	<i>Axxxs</i>	0	13.3
			<i>Qxsss</i>	0	11.2	<i>Axxaa</i>	0	13.5
			<i>Qasax</i>	0	17.3	<i>Axaxs</i>	0	13.5
			<i>Qassx</i>	0	20.3	<i>Aasxx</i>	0	14.7
			<i>Qaaxa</i>	1	24.2	<i>Axxas</i>	0	15.1
			<i>Qaaxs</i>	1	25.0	<i>Axsax</i>	0	17.8
			<i>Qaasx</i>	1	28.7	<i>Axxsx</i>	0	22.2
			<i>Qaaa</i>	1	28.7	<i>Aaaxx^c</i>	0	23.6
						<i>Aaxxs</i>	0	48.0
						<i>Aaxxa^c</i>	0	48.7

^a Number of imaginary frequencies. ^b Energies are relative to the most stable conformer for each series once it has been corrected with ZPVE. These references are $E(+ZPVE)(Casaa) = -953.92802$ au, $E(+ZPVE)(Qaxsa) = -953.53752$ au, and $E(+ZPVE)(Asxxx) = -953.03173$ au. ^c ω_1 differs from 180.0° by less than 0.2°. ^d ω_5 differs from 0.0° by less than 0.1°. ^e $\omega_5 = 0.7^\circ$. ^f *As-* rotamers are not planar; main distortions from the planar geometry are *Asxxx* ($\omega_1 = -20.7^\circ$, $\omega_3 = 0.4^\circ$, $\omega_5 = -20.7^\circ$), *Asxax* ($\omega_1 = -20.6^\circ$, $\omega_3 = -179.8^\circ$, $\omega_5 = -21.4^\circ$), *Asxxx* ($\omega_1 = -21.1^\circ$, $\omega_2 = 1.0^\circ$, $\omega_5 = -20.9^\circ$), *Asaxx* ($\omega_1 = -20.9^\circ$, $\omega_2 = -161.2^\circ$, $\omega_5 = -20.6^\circ$).

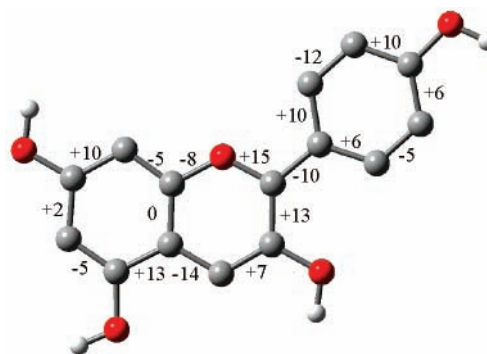


Figure 3. Relative bond lengths in the most stable form of cationic pelargonidin with regard to the flavylium cation. All values in Å multiplied by 10³. B3LYP/6-31++G(d,p) optimized geometry for the flavylium cation is listed as supporting information.

The large energy difference between *Caa--* and *Cas--* conformers may be due to the high repulsion among coplanar hydrogens H3, H4, and H5 which is slightly reduced when H5 leaves the molecular plane. Interatomic distances show that the energy preference for *Cas--* over *Caa--* is due to steric interactions. Thus, for example, *Caaaa* displays H4...H5 and H3...H4 distances of 2.055 and 2.265 Å, respectively, whereas the shortest interatomic distances in *Casaa* are 2.389 Å (H5...H6) and 2.300 Å (H3...H4). Moreover, O5 moves away from H4, opening C10–C5–O 7.7° wider in *Caaaa* (123°) than in *Casaa* and closing O–C5–C6 7.6° in *Caaaa* (116.8°) with regard to *Casaa*. In contrast, no important differences are observed for bond distances (none of them exceeds 0.007 Å).

When the geometry of the cationic form of pelargonidin is compared to that of the parent flavylium cation (all OH groups replaced by hydrogens), it can be observed (Figure 3) that C2–

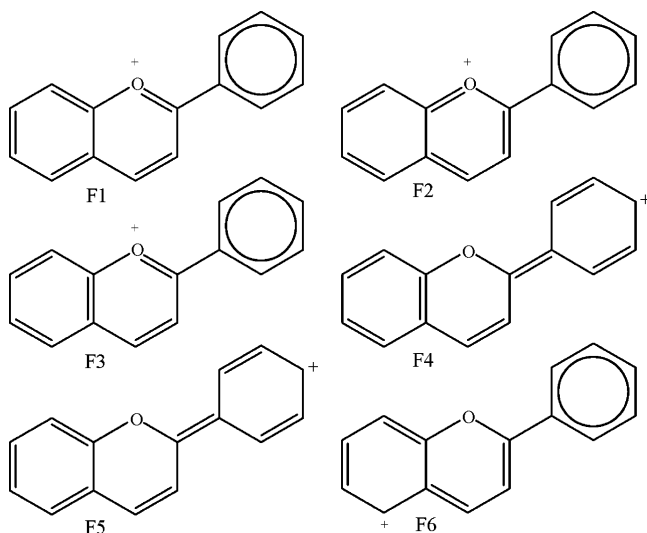


Figure 4. Some significant resonance structures for flavylium cation. Other resonance structures (not shown) place the positive charge on C2, C4, C5, C7, C9, C2', C6'.

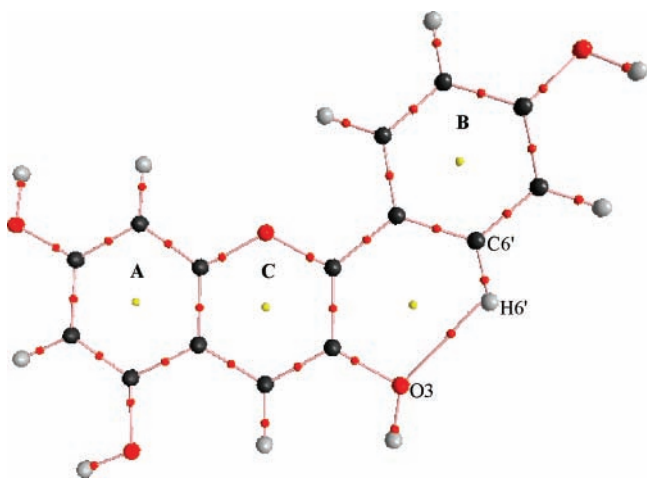


Figure 5. Pelargonidin cation molecular graph (obtained with AIM-2000⁵²) for its most stable rotamer computed from its completely optimized B3LYP/6-31++G(d,p) electron density. The molecular graph contains the bond path associated to the O3...H6'–C6' IHB.

C1' bond length shrinks from 1.450 Å (flavylium cation) to 1.440 Å, whereas O1–C2 lengthens from 1.337 Å (flavylium cation) to 1.351 Å and C2–C3 also lengthens from 1.409 Å (flavylium cation) to 1.422 Å. This has been explained in terms of the resonance model considering that the introduction of one OH group in 4' stabilizes the carbocation represented by structures F4 and F5 in Figure 4. Nevertheless, introduction of the OH group in 5 should stabilize resonance form F6 leading to the lengthening of C5–C10 and C5–C6. Figure 3 shows that the latter is contradicted by the optimized structures.

The electron density analysis carried out with the quantum theory of atoms in molecules (QTAIM)³¹ indicates by finding a bond path (Figure 5) that the eight rotamers (four *Cas*- conformers and four *Caa*- transition states) display an intramolecular hydrogen bond (IHB) connecting O3 and H6', O3...H6'–C6', as assumed in previous papers by Pereira et al.^{19,21} We observe that the frequency which can be assigned to C6'–H6' vibration, $\nu(\text{C6}'\text{--H6}')$, is 3284.3 cm⁻¹ (in *Casa* and displaying very slight variations for the other conformers of pelargonidin cation) and is 3222.1 cm⁻¹ in the equivalent conformer of the 3-deoxy-pelargonidin structure (apigeninidin),

which obviously does not present this IHB. Also, the C6'–H6' bond length is shorter in pelargonidin (1.079 Å) than in apigeninidin (1.084 Å), indicating the formation of a blue-shifted IHB.

Overall, we can say that the conformational energy of the cations is mainly determined by ω_2 (the energy rises around 20 kJ mol⁻¹ when this dihedral goes from syn to anti arrangement) and ω_1 (which prefers the anti orientation over the syn by more than 8 kJ mol⁻¹). In contrast, ω_3 and ω_4 have a much smaller effect on the conformational energy, raising the energy by 1.7 and 1.1 kJ mol⁻¹, respectively, when passing from anti to syn dispositions. The internal rotation around C2–C1' is significantly hindered although the molecular energy remains practically constant along the interval $-20^\circ \leq \omega_5 \leq 20^\circ$ (Figure 2c).

The eight stationary points found in gas phase were also optimized with no restrictions simulating the aqueous solvation with the PCM method. All the optimized structures show at least one imaginary frequency (two when the corresponding gas-phase structure is a saddle point). The new imaginary frequency, observed for the eight rotamers, represents a movement that can be described approximately as an internal rotation around the C2–C1' bond and will be named $\nu(\text{C2--C1}')$ in what follows.

To find the real minima, we have tried several things like performing subsequent unrestricted optimizations with more rigorous convergence criteria and computing relaxed scans of ω_1 and ω_5 . All of these procedures were unsuccessful for locating the true minima. The most detailed minimum search, carried out for the *Casa* conformer, included 1° stepwise relaxed scan of two dihedral angles (ω_1, ω_5). The profile of the PCM energy surface obtained for rotating ω_1 is significantly flat between 0 and 10° as shown in the detail in Figure 2a. The lowest molecular energy achieved was 0.2 kJ mol⁻¹ more negative than the planar structure. This energy difference is clearly below the confidence level of DFT calculations. Moreover, $\nu(\text{C2--C1}')$ is imaginary for this optimized nonplanar structure. Taking into account that the modulus of $\nu(\text{C2--C1}')$ is rather small (around 17 cm⁻¹) and the shortcomings associated to frequency calculations within the framework of PCM,³² we assume that the exact position of the four expected minima cannot be determined by this method. Actually, the concrete positions of these conformers are not really important as they are experiencing large amplitude vibrations in this flat region of ω_1 and ω_5 . Finally, we think that the planar *C* structures are not true minima for PCM optimizations. In fact, the moduli of the imaginary $\nu(\text{C2--C1}')$ computed for them are larger than 30 cm⁻¹.

In summary, we can say that (1) solvated *Cas*- conformations are found around 12 kJ mol⁻¹ more stable than their corresponding *Caa*- conformations and (2) the most stable conformations (Table 2) of the solvated cation, *Casa*, are not planar, as reflected by two of the main dihedral angles ($\omega_1 = 176.6^\circ$ and $\omega_5 = 13.6^\circ$, Figure 2).

Quinonoidal Forms. The flavylium cation analogue studied above is the main form in strong acidic media. Anthocyanin cations are transformed into neutral quinonoidal forms upon deprotonation when raising the pH. Hydroxylic hydrogens are obviously the most suitable targets for deprotonation. Therefore, one OH group is replaced by a carbonyl in these forms. As pelargonidin has four –OH groups, we can distinguish four different quinonoidal tautomers (Figure 6), which henceforth will be named by the atom attached to the carbonyl oxygen. Every one of them appears as a set of rotamers. After checking

TABLE 2: B3LYP/6-31++G(d,p) Relative Energies (in kJ mol⁻¹) for PCM Modeled Aqueous Solvated Pelargonidin Rotamers

rotamer	ω_1	ω_2	ω_3	ω_4	ω_5	ΔG_{solv}^a	E_{pol}^a	$E^{\text{PCM}} - E^{\text{gas } a}$	ΔE^b
<i>Casas</i> ^c	180.0	0.1	180.0	0.1	0.0	-65.8	-75.4	-69.0	0.0
<i>Casaa</i> ^d	179.9	0.1	180.0	180.0	0.6	-65.3	-74.9	-68.7	0.0
<i>Casss</i> ^d	179.8	0.2	0.2	0.1	0.9	-66.5	-76.1	-69.2	0.4
<i>Cassa</i> ^d	180.0	0.1	0.1	180.0	0.1	-66.3	-75.8	-69.0	0.5
<i>Caaaa</i> ^e	179.9	180.0	180.0	180.0	0.2	-69.4	-79.1	-71.1	14.7
<i>Caaas</i> ^e	179.9	179.8	180.0	0.1	0.0	-69.7	-79.4	-71.3	14.7
<i>Caass</i> ^e	180.0	180.0	0.1	0.1	0.1	-68.7	-78.4	-70.6	14.8
<i>Caasa</i> ^e	180.0	180.0	0.1	180.0	0.1	-68.6	-78.3	-70.5	14.8
<i>Qasxs</i>	173.6	0.0	x	0.2	15.8	-37.0	-47.0	-34.9	0.0
<i>Qasxa</i>	173.5	0.1	x	179.6	16.3	-37.3	-47.3	-34.9	0.2
<i>Qaxss</i>	174.0	x	0.1	0.0	16.5	-32.9	-42.9	-33.3	0.5
<i>Qaxsa</i>	174.2	x	0.2	179.9	15.7	-32.9	-42.9	-33.2	0.7
<i>Qaxaa</i>	174.3	x	179.1	0.1	16.6	-36.1	-46.1	-34.6	2.5
<i>Qaxas</i>	174.2	x	179.5	0.1	15.9	-36.1	-46.1	-34.7	2.5
<i>Qxsaa</i>	x	0.1	180.0	180.0	-0.3	-34.4	-44.4	-34.2	2.8
<i>Qxsas</i>	x	0.1	180.0	0.1	0.0	-35.9	-45.8	-34.8	2.9
<i>Qxssa</i>	x	0.1	0.2	180.0	0.0	-35.8	-45.8	-34.9	3.7
<i>Qxsss</i>	x	0.1	0.2	0.1	-0.7	-37.1	-47.1	-35.4	3.8
<i>Qasax</i>	179.9	0.1	179.9	x	0.1	-42.0	-51.9	-36.4	5.0
<i>Qasxx</i>	179.9	0.1	0.2	x	0.2	-44.0	-53.9	-37.2	5.4
<i>Qxaaa</i>	x	179.7	179.9	180.0	0.2	-30.7	-40.8	-31.9	14.1
<i>Qaaxs</i>	174.4	147.7	x	0.2	16.3	-41.2	-51.3	-35.4	14.2
<i>Qxaas</i>	x	179.8	179.9	0.1	-0.6	-32.0	-42.1	-32.5	14.2
<i>Qaaxa</i>	174.0	148.1	x	179.5	16.4	-41.6	-51.7	-34.3	14.4
<i>Qxasa</i>	x	178.5	0.1	179.9	-0.1	-30.4	-40.5	-31.8	14.6
<i>Qxass</i>	x	180.0	0.1	0.1	0.2	-31.6	-41.7	-32.3	14.7
<i>Qaasx</i>	180.0	179.9	0.1	x	0.0	-43.4	-53.4	-36.6	17.7
<i>Qaaaax</i>	180.0	179.9	180.0	x	0.0	-43.1	-53.1	-36.6	17.7
<i>Axxsa</i>	x	x	0.1	179.9	-0.3	-69.7	-80.0	-66.8	0.0
<i>Axxss</i>	x	x	0.1	-0.1	-0.3	-70.7	-81.1	-67.2	0.0
<i>Aaxsx</i>	176.6	x	0.2	x	2.1	-65.4	-75.7	-64.6	0.5
<i>Axxxs</i>	x	0.1	x	-0.1	-0.3	-69.1	-79.4	-67.5	0.8
<i>Axxsa</i>	x	0.2	x	179.9	0.1	-68.5	-78.8	-67.2	0.9
<i>Axxaa</i>	x	x	180.0	179.9	-0.1	-72.0	-82.4	-67.6	1.3
<i>Axxas</i>	x	x	180.0	-0.1	-0.2	-73.2	-83.6	-68.1	1.4
<i>Aasxx</i>	180.0	0.1	x	x	0.2	-70.9	-81.2	-66.9	2.2
<i>Aaxax</i>	178.7	179.9	x	x	0.6	-67.0	-77.3	-65.2	2.3
<i>Axsax</i>	x	0.1	180.0	x	0.2	-73.7	-84.0	-68.4	2.4
<i>Axssx</i>	x	0.0	0.2	x	0.3	-76.1	-86.4	-69.5	3.1
<i>Aaxxs</i>	172.5	x	x	0.1	17.9	-81.2	-91.5	-74.7	6.3
<i>Aaxxa</i>	173.8	x	x	-179.5	16.7	-81.6	-91.9	-74.9	6.5
<i>Axxsx</i>	-62.1	x	0.3	x	-15.8	-63.6	-74.1	-62.1	8.8
<i>Axxsx</i>	-68.4	0.8	x	x	-13.3	-66.8	-77.2	-63.4	9.4
<i>Axxax</i>	-69.8	x	-179.7	x	-12.8	-65.6	-76.0	-62.7	10.5
<i>Axxax</i>	x	-180.0	-180.0	x	0.1	-66.7	-77.2	-63.6	11.5
<i>Axxsx</i>	x	-179.8	0.1	x	0.0	-67.5	-77.9	-63.9	11.9
<i>Axxsx</i>	x	177.3	x	0.0	0.7	-66.5	-77.0	-65.1	12.5
<i>Axxax</i>	x	-179.7	x	-180.0	0.3	-66.0	-76.5	-64.9	12.6
<i>Aaaxx</i>	179.9	179.8	x	x	0.3	-73.7	-84.0	-67.3	15.6
<i>Asaxx</i>	-69.6	-153.8	x	x	-12.2	-67.6	-78.1	-62.7	21.3

^a Values in kcal mol⁻¹. ΔG_{solv} , E_{pol} , and $E^{\text{PCM}} - E^{\text{gas}}$ represent, respectively, the solvation Gibbs energy, the PCM term for polarization energy, and the difference between electronic molecular energies for PCM and isolated molecule calculations. ^b Energies are relative to the most stable conformer for each series once it has been corrected with ZPVE. These references are $E(+\text{ZPVE})(\text{Casas}) = -954.04449$ au, $E(+\text{ZPVE})(\text{Qasxs}) = -953.59521$ au, and $E(+\text{ZPVE})(\text{Axxsa}) = -953.13721$ au. ^c The actual geometry for the *Casas* conformation with the most negative energy displays $\omega_1 = 176.6^\circ$, $\omega_2 = -0.2$, $\omega_3 = -179.4$, $\omega_4 = 0.1$, and $\omega_5 = 13.6$. ^d It is expected that this conformation is a transition state very close in energy to the real conformer as obtained for *Casas*. Results obtained for *Casas* (Figure 3) indicate that the computational cost for obtaining the true minima is not justified. Therefore, we have assumed that the PCM energy of the four *C* minima can be represented by that of the corresponding planar form, and these are the data shown this table. ^e These structures display two imaginary frequencies, one associated to ω_2 (already displayed by the corresponding gas-phase structure) and another to ω_5 . According to the behavior shown by *Casas*, the actual transition state should display similar geometry (but nonplanar) and very close energy.

again that antiperiplanar dispositions of ω_1 are of lower energy than the corresponding synperiplanar ones (Supporting Information), four different rotamers were studied for C4', C7, and C5 tautomers and eight were studied for C3.

C5 tautomer is found as the most stable one with two rotamers that are nearly isoenergetic (*Qaxsa* and *Qaxss*). The remaining rotamers of C5 (*Qaxaa* and *Qaxas*) are slightly destabilized (7.0 and 7.3 kJ mol⁻¹, respectively). The most important difference between interbonded distances is that observed for the H5...H closest nonbonded distance (2.29 Å for the former and 2.26 Å

for the latter). This difference cannot be responsible for relative energies of 7.0 kJ mol⁻¹, and in fact, it gives rise to less than 0.3 kJ mol⁻¹ according to Allinger et al.'s MM3³³ van der Waals term of this molecular mechanics force field.³⁴ In contrast, there is a very significant variation of global dipole moment when ω_3 is rotated, going from 5.3 D in *Qaxsa* (5.0 D in *Qaxss*) to 7.8 D in *Qaxaa* (7.7 D in *Qaxas*), pointing to an electrostatic origin for this destabilization.

There is a group of rotamers of the C5, C3, and C7 tautomers whose energies are between 6 and 11 kJ mol⁻¹ less negative

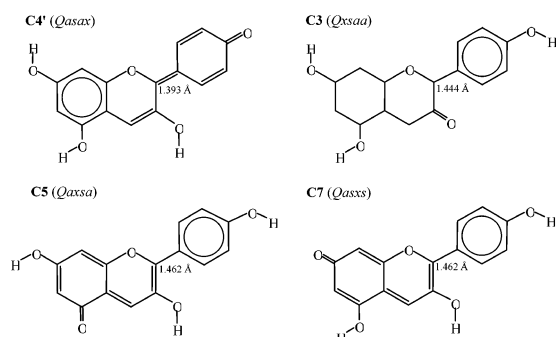


Figure 6. Tautomers of the quinonoidal form of pelargonidin in their most stable conformers (name in parenthesis) represented by their uncharged canonical Lewis structures excluding C3 where no uncharged Lewis structure can be drawn.

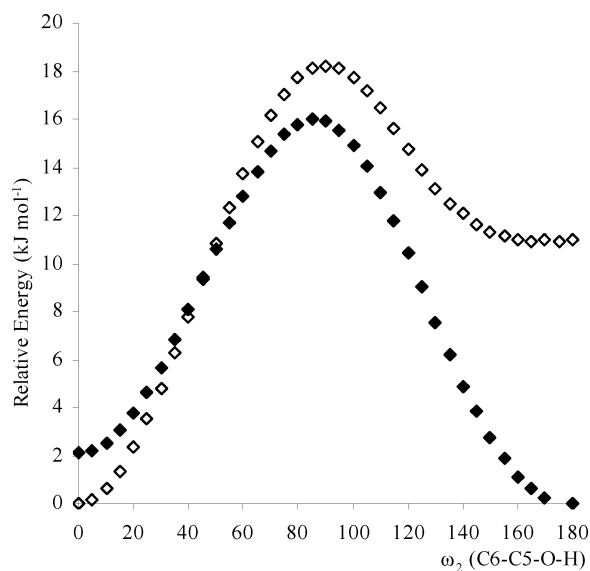


Figure 7. Energy profiles for the internal rotation around ω_2 (C6–C5–O–H) for isolated and PCM modeled aqueous solution of C3 tautomer (interconversion between $Qxss$ and $Qxass$ rotamers). Bold face symbols refer to isolated molecule and open face symbols refer to PCM calculations.

than that of $Qaxsa$. In contrast, all the rotamers of the $C4'$ tautomer display relative energies larger than 17 kJ mol^{-1} (Table 1). Computed frequencies indicate that four rotamers of different tautomers are transition states. All of them show simultaneous antiperiplanar disposition of ω_2 and ω_1 ($Qaa--$ in Table 1). In contrast to what has been found for the cation and the remaining tautomers of the quinonoidal form, the relative energies of the rotamers of the C3 tautomer cannot be classified using ω_2 values. In fact, the anti arrangement of ω_2 is preferred in two pairs of rotamers ($Qx-ss$ and $Qx-sa$), as shown in Figure 7, whereas the other two pairs prefer the syn arrangement as was found for the cation.

All the rotamers, both true minima and transition states, are completely planar. Tautomerism gives rise to important variations in the bond lengths of the polycyclic system (Table 3), which are practically unaffected by internal rotation of hydroxyls and which basically agree with the predictions that can be inferred from the resonance model looking at the structures drawn in Figure 6. Thus, referring the bond lengths of the quinonoidal tautomers to the corresponding ones in the most stable cationic rotamer ($Casaa$), we observe that (1) C5 and C7 tautomers have bond lengths that are significantly different from those of the cation in the **AC** bicycle, whereas they are practically equivalent in ring **B**; (2) all the bond lengths of the

TABLE 3: B3LYP/6-31++G(d,p) Optimized Main Bond Lengths^a for the Most Stable Cation^b and Every Tautomer^c of Quinonoidal^c Isolated Pelargonidin

	$C4'$ tautomer <i>Casaa</i>	C7 tautomer <i>Qasax</i>	C5 tautomer <i>Qaxsa</i>	C3 tautomer <i>Qxaaa</i>
C5–C6	1.379	0.011	−0.021	0.059
C6–C7	1.415	−0.011	0.059	−0.034
C5–C10	1.430	−0.017	0.015	0.065
C9–C10	1.413	−0.011	0.032	0.020
C4–C10	1.405	0.028	−0.033	−0.035
C8–C9	1.389	0.005	−0.029	−0.021
C7–C8	1.399	−0.003	0.058	0.029
C3–C4	1.385	−0.021	0.032	0.030
C2–C3	1.422	0.029	−0.040	−0.037
C2–C1'	1.440	−0.047	0.022	0.022
C1'–C2'	1.425	0.028	−0.012	−0.010
C1'–C6'	1.421	0.030	−0.006	−0.009
C2'–C3'	1.377	−0.020	0.012	0.010
C5'–C6'	1.384	−0.025	0.005	0.008
C3'–C4'	1.410	0.058	−0.009	−0.009
C5'–C4'	1.406	0.059	−0.007	−0.007
C2–O1	1.351	0.029	0.017	0.015
C9–O1	1.343	0.019	0.030	0.027

^a All values in Å. ^b Absolute values. ^c Values are relative to those of *Casaa*.

tautomer $C4'$ in the **AC–B** system (excluding C7–C8 and C8–C9) show important changes with regard to the cation; and (3) only two bond lengths (C2–C3 and C3–C4) of the tautomer C3, which cannot be represented by any uncharged Lewis structure, are significantly different to those of the cation.

The only remarkable changes observed for bond angles within the polycyclic skeleton are localized in the C–C–C angle, θ , whose central carbon is attached to the deprotonated OH. These angles close between 6° (C5 and C3 tautomers) and 5° ($C4'$ and C7 tautomers) upon hydrogen abstraction with regard to their value in the corresponding cation (Supporting Information). There are also bond angles involving H or O atoms that experience significant modifications in the series of quinonoidal tautomers. They can be related to the cycle geometry reorganization accompanying θ closing.

All the quinonoidal rotamers display (as commented above for the cation) the $O3 \cdots H6' - C6'$ hydrogen bonding (detected as a QTAIM bond path). According to interatomic distances and to the electron density at the corresponding bond critical point (BCP), ρ_{BCP} , this IHB becomes stronger when O3 is in sp^2 hybridization (tautomer C3). Thus, ρ_{BCP} rises from $1.87 \cdot 10^{-2}$ au in the other tautomers to $2.45 \cdot 10^{-2}$ au in C3 and $R_{O3-H6'}$ displays the smallest value in the series in C3 (2.057 \AA). The blue-shift for $C6' - H6'$ becomes negligible in C3 ($\nu_{C-H} = 3229.9 \text{ cm}^{-1}$, $R_{C-H} = 1.083 \text{ \AA}$), whereas it is still significant in the other tautomers ($3269.9 \text{ cm}^{-1} < \nu_{C-H} < 3271.6 \text{ cm}^{-1}$; $R_{C-H} = 1.080 \text{ \AA}$). All the rotamers, if we exclude those of the C3 tautomer, display also another hydrogen bond ($O1 \cdots H2' - C2'$) which, according to QTAIM analysis, is weaker ($\rho_{BCP} = 1.62 \cdot 10^{-2}$ au).

Another common characteristic of quinonoidal rotamers is a high dipole moment. All of them are above 4.9 D if we exclude the $Qxasa$ and $Qxaaa$ (2.45 and 3.84 D, respectively), and it is 5.33 D for the most stable rotamer, $Qaxsa$.

All the rotamers of C5 and C7 tautomers lose the planarity obtained for gas phase after PCM optimization, although the energy difference with the planar structure (obtained as a transition state) is very small (never larger than 0.5 kJ mol^{-1}). The remaining tautomers ($C4'$ and C3) keep the planarity because of the importance of the C2–C1' double-bonded

resonance form in C4' and because of the enhancement of O3...H6'-C6' IHB after abstraction of H3 in C3. PCM frequency calculation finds for some planar structures (all C5 and C7 tautomers) one imaginary frequency (associated to the internal rotation around C2-C1') that is not obtained in the gas phase. In this case, we have obtained true nonplanar minima when the optimizations were carried out without any symmetry restrictions. Table 2 lists the main characteristics of completely optimized geometries.

Another result of PCM optimizations is a general reduction of relative conformational energies. Thus, two rotamers of C7 (*Qaxsx* and *Qasxa*) and two of C5 (*Qaxss* and *Qaxsa*), those with synperiplanar dispositions of ω_2 , are found as the most stable rotamers and their energies differ by less than 1 kJ mol⁻¹. Also, the C5 rotamers showing antiperiplanar disposition of ω_3 display relative energies below 2.5 kJ mol⁻¹. The most significant change in relative energy takes place when ω_2 is antiperiplanar. This disposition raises the relative energy above 14 kJ mol⁻¹. Nevertheless, these relative energies are smaller than those obtained in gas phase (Tables 1 and 2).

All the rotamers of tautomer C4' are significantly stabilized in PCM with regard to gas phase, whereas the opposite trend is followed by the *Qxa--* rotamers of tautomer C3. The most negative polarization energy between solute and solvent is obtained for C4' rotamers (-51.9 to -53.9 kcal mol⁻¹) and C7 rotamers with antiperiplanar ω_2 (-51.2 to -51.7 kcal mol⁻¹). This can be related to the long distance between the most negative and positive sites of the molecule (carbonyl oxygen and hydroxyl hydrogens, respectively), which allows the spreading of a higher charge density over their neighborhoods on the cavity surface. In fact, when the 5-OH of C7 becomes synperiplanar (approaching hydroxyl H5 at one side of carbonyl O7), the polarization term is reduced (-47.0 to -47.3 kcal mol⁻¹). In the same vein, the smallest polarization energies (-40.5 to -42.1 kcal mol⁻¹) are shown by *Qxa--* where the carbonyl group at C3 is very close to hydroxylic H5. This explains why these rotamers are relatively destabilized in PCM.

Anionic Forms. Neutral quinonoidal forms are transformed into anions upon deprotonation of another hydroxyl in basic media. We are naming the diverse anion tautomers indicating the atoms attached to the two carbonyl oxygens. Again, there is a series of rotamers for every tautomer. In this case, the assumption that synperiplanar dispositions of ω_1 are of higher energy than the corresponding antiperiplanar ones is not correct for all the tautomers. Thus, the reverse trend is found for C7C4' and C5C4' tautomers (Supporting Information). Therefore, we have studied four different rotamers for C3C5 (*Axxsa*, *Axxss*, *Axxas*, *Axxaa*), C3C7 (*Axxsa*, *Axxss*, *Axaxs*, *Axaxa*), C3C4' (*Axxsx*, *Axaxs*, *Axaax*, *Axsax*), C5C4' (*Aaxsx*, *Aaxax*, *Asxxs*, *Asxax*), and C7C4' (*Aaaxx*, *Aasxx*, *Asaxx*, *Assxx*) tautomers and two rotamers for C5C7 (*Aaxxs*, *Aaxxa*).

C5C4' is the most stable tautomer, displaying in gas phase a significant preference for the nonplanar *Asxxs* rotamer (Table 1). The following tautomer in the stability sequence is C3C4', but the relative energy of its rotamers depends highly upon the disposition of ω_2 , the antitautomers being more than 10 kJ mol⁻¹ more stable than the syn. If we exclude the *Axxs-* rotamers of tautomer C3C5, the relative energies of the remaining rotamers are over 10 kJ mol⁻¹. The C5C7 tautomer also has high relative energy (Table 1).

As was found for quinonoidal forms, tautomerism gives rise to important variation in the bond lengths of the polycyclic system, which are practically unaffected by internal rotation of hydroxyls (see below for exceptions) and which agree with the

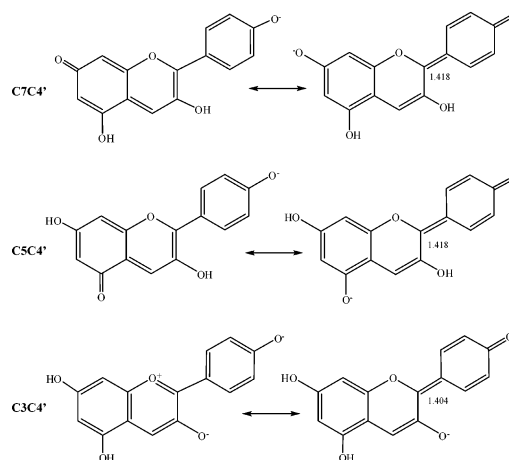


Figure 8. Main canonical forms for the diverse C4' deprotonated tautomers of pelargonidin. C2-C1' bond lengths shown for C7C4' and C5C4' tautomers correspond to *Aa---*rotamers (planar). They lengthen by 0.010 Å in the corresponding *As---*rotamer.

resonance model (Supporting Information). Thus, C2-C1' is significantly shorter in those tautomers involving O4' deprotonation (1.418–1.428 Å in C5C4' and C7C4' and 1.404 in C3C4') than in the remaining ones (1.450 Å in C3C5 and C3C7 and 1.465 Å in C5C7). There are canonical forms assigning a C2=C1' formal double bond in the first series, whereas all the canonical forms of the second series leave formal single bonds for C2-C1'. Moreover, the shortest C2-C1' bond lengths correspond to the C3C4' tautomer where the unique Lewis structure leaves a formal double bond for C2=C1'. The fact that C2-C1' bond length in C5C4' and C7C4' tautomers is closer to that of the formal double bond than to the single one can be related to a preference for canonical forms A2 (Figure 8). (For more details, see Supporting Information, Figure S1.) This preference is supported by QAIM atomic electron populations, which are higher for deprotonated oxygens of the AC bicycle (9.225–9.239 au) than for deprotonated O4' (9.209–9.214 au). Significant variations observed for other bond lengths across the tautomers (Supporting Information, Table S3) are also explainable in relation to resonance structures.

The only significant variation of the geometry due to internal rotation around C-OH bonds is obtained when ω_1 is rotated from anti- to synperiplanar disposition. Thus, when planar *Aaxsx* interconverts into the nonplanar *Asxxs* conformer, C2-C1' lengthens and C2-C3 shortens by 0.01 Å. This geometry change allows a reduction of electron-electron repulsions between H3 and H6'.

All the anionic rotamers disposing ω_1 in *a* arrangement display (as commented above for cation and neutral forms) the O3...H6'-C6' hydrogen bonding (detected as a bond path). This interaction is not present in the corresponding *s* rotamers (the most stable for C5C4' and C7C4' tautomers). Interatomic distances and ρ_{BCP} values indicate that this IHB is stronger when O3 is deprotonated (tautomers C3-). Thus, ρ_{BCP} is between $2.31 \cdot 10^{-2}$ and $2.34 \cdot 10^{-2}$ au in these tautomers and goes from $1.80 \cdot 10^{-2}$ to $1.90 \cdot 10^{-2}$ au when O3 is protonated (tautomers C5C4', C5C7, and C7C4'). $R_{O3-H6'}$ is shorter than 2.090 Å for O3 deprotonated forms and is longer than 2.137 Å for the O3 protonated ones. In all cases, $\nu_{C6'-H6'}$ frequencies are lower with regard to their values in quinonoidal forms. Accordingly, C6'-H6' bond lengths are longer in the anion than in the corresponding rotamer of the neutral form. Although $\nu(C6'-H6')$ is still blue-shifted with regard to apigenidin for the most stable tautomer, tautomers where H has been abstracted from C3 show red-shifted $\nu(C6'-H6')$ (e.g., 3212.9 cm⁻¹ for C3C7). Finally,

O1...H2'-C2' IHB is only observed in C5C7, being weaker than O3...H6'-C6' ($\rho_{\text{BCP}} = 1.65 \cdot 10^{-2}$ au and $R_{\text{O1-H2}'} = 2.290$ Å).

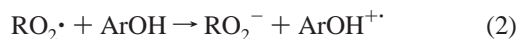
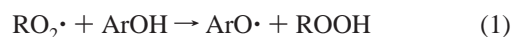
The rotamers of C5C7 and C5C4' tautomers lose the planarity obtained for gas phase after PCM optimization with ω_5 around 17° and 2.1° , respectively. The energy difference with the planar structures (obtained as a transition state with one imaginary frequency always larger than $30i$ cm $^{-1}$ and associated to the internal rotation around C2-C1') is very small (never larger than 0.5 kJ mol $^{-1}$). The remaining tautomers keep the planarity.

Tautomers with a carbonyl group at C3 display the lowest energy according to PCM optimizations if we exclude those rotamers where ω_2 is antiperiplanar. As usual, the conformational energy interval gets narrow after PCM optimizations. Thus, 11 rotamers show relative energies below 1 kcal mol $^{-1}$. They represent five different groups of tautomers (C3C5, C5C4', C3C7, C7C4', and C3C4'). The largest relative energies correspond to *Aaaxx* (where the hydroxylic H3 and H5 are quite close to H4) and to *Axa--* rotamers where, as commented for the quinonoidal forms, the relative orientations of the carbonyl at C3 and the hydroxyl at C5 are not compatible with optimum solvation. Once more, we find that the most significant change in relative energy takes place when ω_2 is antiperiplanar. This disposition raises the relative energy above 10 kJ mol $^{-1}$. Nevertheless, these relative energies are smaller than those obtained in gas phase (Tables 1 and 2).

The rotamers of tautomer C5C7 (*Aaxxs* and *Aaxxa*) are the most stabilized in PCM with regard to the gas phase (-74.7 and -74.8 kcal mol $^{-1}$) because of its high polarization (-91.5 and -91.9 kcal mol $^{-1}$) and solvation (-81.2 and -81.6 kcal mol $^{-1}$) energies, whereas the opposite trend is followed by the *Axa-* rotamers (Table 2).

Ionization Potential and O-H Bond Dissociation Energies.

Anthocyanins are polyphenolic antioxidants (ArOH) since they contain at least one hydroxyl group attached to a benzene ring. They intercept free radicals, reacting with them at a faster rate than the substrate. Since free radicals are able to attack a variety of targets including lipids, fats, and proteins, it is believed that they are implicated in several important degenerative diseases including aging itself.³⁵⁻³⁸ It is commonly accepted that the key factors that help to enhance the antioxidant activity of polyphenols include¹⁵ (1) a relatively low O-H bond dissociation enthalpy (BDE), which facilitates the H-abstraction reaction with the radical (eq 1), and (2) a relatively high ionization potential (IP) that decreases the electron-transfer rate between antioxidant and oxygen that yields ArOH⁺ cations (eq 2). Radical cations are potential pro-oxidative species, which have been shown to undergo substitution on DNA bases and which thereby exert mutagenic effects.³⁹ Nevertheless, it has been also reported that low IPs may enhance antioxidant activity when the formation of ArOH⁺ is followed by the proton transfer shown in (eq 3).⁴⁰



IPs were calculated in the gas phase for the most stable structure of cation, neutral, and anion forms of isolated pelargonidin taking into account zero point vibrational energies (ZPVEs) and thermal corrections to enthalpy (TCEs). It can be observed that the IP of pelargonidin diminishes when H-abstraction progresses reducing the number of OH groups in

TABLE 4: Ionization Potential (IP) and O-H Bond Dissociation Energies (BDE), in kJ mol $^{-1}$, for the Most Stable Rotamer of the Three Forms of Isolated Pelargonidin

	BDE				IP
	3OH	5OH	7OH	4'OH	
<i>Casaa</i>	339.3	366.6	375.3	381.6	1031.0
<i>Qasxs</i>	287.8	x	346.5	327.5	644.5
<i>Asxss</i>	255.5	x	323.3	x	320.4

the molecule (Table 4). This differs with previously reported results, where a growing number of OH in the molecule results in lower IP.^{41,42} The reason is because in previous cases the comparison was established among neutral forms of similar compounds (sets of hydroxybenzoic⁴¹ and cinnamic⁴² acids) and here we are studying cationic, neutral, and anionic forms of the same molecule. Therefore, the expected sequence for IPs is cation > neutral > anion. Anyway, according to eq 2, acid pH enhances pelargonidin antioxidant activity.

The cation of pelargonidin can be considered as a very powerful antioxidant species as its IP is significantly larger than widely used food synthetic additives as butylated hydroxyanisole, propyl gallate, and nordihydroguaiaretic acid (639 , 702 , and 672 kJ mol $^{-1}$, respectively)¹⁵ and the natural flavanoid antioxidants epigallocatechin-3-gallate (618 kJ mol $^{-1}$), one of the most active antioxidants obtained from green tea,⁴³ epicatechin (714.8 kJ mol $^{-1}$),⁴⁰ tocopherol (648.1 kJ mol $^{-1}$),⁴⁴ or quercetin (694.9 kJ mol $^{-1}$).⁴⁵ Even the IP of neutral pelargonidin can be satisfactorily compared (644 kJ mol $^{-1}$) to most of those indicated above.

BDE was calculated in the gas phase for each OH group of the most stable cation (*Casaa*), quinonoidal (*Qasxa*), and quinonoidal-anion (*Asxss*) forms of pelargonidin in the gas phase. For this calculation, we have also included ZPVE and TCE corrections. BDE is calculated as the enthalpy difference at 298 K for eq 4, where ArOH is the parent polyphenol and ArO \cdot is the corresponding polyphenoxy radical.



BDEs computed are smaller (254.1 – 339.3 kJ mol $^{-1}$) than those of hydroxybenzoic acids (350 – 442 kJ mol $^{-1}$)⁴¹ and phenol (values varying from 346 to 360 kJ mol $^{-1}$ depending upon the method employed).⁴⁶ Most of them are also lower than the BDE computed by Zhang and Ji for 2,2,5,7,8-pentamethyl-6-hydroxychroman (325.9 kJ mol $^{-1}$),⁴⁷ a model compound for vitamin E. Analyzing the position of broken OH, we observe that 3 is the most labile position. This can be explained considering the presence of an IHB between O3...H6'-C6'. As this position is usually glycosidated in anthocyanins, other BDEs shown in Table 4 for each form should also be considered for analyzing the antioxidant activity of natural compounds. It is also noticeable that BDE computed for each position follows the sequence cation > neutral > anion. Therefore, lowering the pH has opposing effects with regard to the antioxidant properties of pelargonidin, raising both IP and BDE.

It is known that the acidity of anthocyanidins exceeds that of other natural polyphenols like flavonoids and hydroxybenzoic acids.^{48,49} Thus, the energies involved in the gas-phase deprotonation processes of the most stable conformers of cationic and neutral pelargonidin (1025.3 and 1328.0 kJ mol $^{-1}$, respectively) are significantly smaller than those computed for a series of natural flavonoids (1456 – 1519 kJ mol $^{-1}$).⁵⁰ It has been stated that the antioxidant mechanism which operated through the chelation of transition-metal ions occurs quite often with at least

one deprotonated ligand.⁵¹ Therefore, relative acidities also point to a higher antioxidant activity of anthocyanidins.

Conclusions

According to our B3LYP/6-31++G(d,p) study, the following conclusions on the conformational equilibria of pelargonidin can be obtained:

1. The most stable conformer of the cationic and neutral forms of pelargonidin is completely planar in the gas phase but is not planar for the anion form.

2. In gas phase, the most stable cations display C2–C3–O–H and C6–C5–O–H anti and syn orientations, respectively. Internal rotations around these units results in very significant destabilizations, whereas syn and anti orientations of hydroxyls at 7 and 4' positions are nearly isoenergetic.

3. C5 is the most stable tautomer of quinonoidal pelargonidin. The energy of this tautomer is significantly affected by the rotation around the C7–O7 bond, displaying a conformational preference for the syn disposition of the C6–C7–O–H dihedral angle. The energies of C3 and C7 tautomers are, at least, 6 kJ mol⁻¹ higher, whereas C4' tautomers can be considered negligible in the conformational mixture as their relative energy exceeds 17 kJ mol⁻¹. C3 tautomers are only 6 kJ mol⁻¹ above the most stabilized ones in spite that it is not possible to write a Lewis structure for their AC system.

4. In gas phase, the most stable tautomers of pelargonidin anion display the two carbonyl groups at C5 and C4'. The rotamers of C3C4' and C3C5 tautomers have relative energies between 6 and 10 kJ mol⁻¹, whereas tautomers with a carbonyl group at C7 display higher energies except for Assxx.

5. Tautomeric equilibria affect substantially the geometries of the AC–B backbone. Thus, the geometries of quinonoidal and anionic pelargonidin display significant changes of C–C bond distances that can be interpreted in terms of resonance forms. Thus, the C2–C1' bond length varies from 1.393 to 1.462 Å in quinonoidal and anionic pelargonidin, contrasting to its constant 1.450 Å value in the cation.

6. All the forms, tautomers, and rotamers with antiperiplanar arrangement of ω_1 in pelargonidin display an intramolecular hydrogen bond between O3 and H6' characterized by a clear blue shift of the frequency associated to C6'–H6' bond in the cation. This frequency gets progressively lower in quinonoidal and anion forms and becomes even red-shifted for the O3-deprotonated tautomers of the anion.

7. The interval of conformational relative energies gets narrow with PCM optimizations, which provide nearly the same conformational sequence for the cation, interchange the relative position of some quinonoidal tautomers, and even alter which is the most stable tautomer in the anion (C3C5 according to PCM and C5C4' in gas phase). PCM calculations also indicate that the planarity is lost in the C5 quinonoidal rotamers, in the C7 tautomers, and in the C5C7 anions.

Finally, gas-phase ionization potentials and O–H BDEs are consistent with an important antioxidant activity.

Acknowledgment. L.E. thanks Universidade de Vigo for a predoctoral fellowship. We also thank "Centro de Supercomputación de Galicia" (CESGA) for free access to its computational facilities.

Supporting Information Available: Geometry details for cation, quinonoidal, and anion forms of pelargonidin and for flavylum cation; energy profiles for the internal rotation around ω_1 (C2–C3–O3–H3) for cation and for the most stable rotamer

of different tautomers of quinonoidal and anion forms of pelargonidin; main resonance structures for the tautomers of pelargonidin anion not shown in Figure 8. This material is available free of charge via the Internet at <http://pubs.acs.org>.

References and Notes

- Mazza, G.; Brouillard, R. *Phytochemistry* **1990**, *29*, 1097.
- Sarma, A. D.; Sharma, R. *Phytochemistry* **1999**, *52*, 1313.
- Meiers, S.; Kemény, M.; Weyand, U.; Gastpar, R.; Von Angerer, E.; Marco, D. *J. Agric. Food Chem.* **2001**, *49*, 958.
- Harbone, J. B.; Grayer, R. J. In *The Flavonoids: Advances in Research since 1980*; Harbone, J. B., Ed.; Chapman and Hall: London, 1988; p 1.
- Brouillard, R. In *The Flavonoids: Advances in Research since 1980*; Harbone, J. B., Ed.; Chapman and Hall: London, 1988; p 525.
- Schwinn, K. E.; Markham, K. R.; Given, N. K. *Phytochemistry* **1994**, *35*, 145.
- Holton, T. A.; Tanaka, Y. *Trends Biotechnol.* **1994**, *12*, 40.
- Lister, C. E.; Lancaster, J. E.; Sutton, K. H.; Walker, J. R. L. *J. Sci. Food Agric.* **1994**, *64*, 155.
- Nessler, C. L. *Transgenic Res.* **1994**, *3*, 109.
- Heredia, F. J.; Franchia-Aricha, E. M.; Rivas-Gonzalo, J. C.; Vicario, I. M.; Santos-Buelga, C. *Food Chem.* **1998**, *63*, 491.
- Brouillard, R. In *Anthocyanins as Food Colors*; Markakis, P., Ed.; Academic Press: New York, 1982; p 1.
- Hall, C. A., III; Cuppett, S. L. In *Antioxidant Methodology*; Aruoma, I. O., Cuppett, S. L., Eds.; AOCS Press: Champaign, IL, 1997.
- Wright, J. S.; Johnson, E. R.; DiLabio, G. A. *J. Am. Chem. Soc.* **2001**, *123*, 1173.
- Pratt, D. A.; DiLabio, G. A.; Brigati, G.; Pedulli, G. F.; Valgimigli, L. *J. Am. Chem. Soc.* **2001**, *123*, 4625.
- Zhang, H. Y.; Sun, Y. M.; Wang, X. L. *Chem. Eur. J.* **2003**, *9*, 502 and references therein.
- Sakakibara, H.; Ashida, H.; Kanazawa, K. *Free Radical Res.* **2002**, *36*, 307.
- Kurtin, W. E.; Song, P. S. *Tetrahedron* **1968**, *24*, 2255.
- Rastelli, G.; Costantino, L.; Albasini, A. *J. Mol. Struct.* **1993**, *279*, 157.
- Pereira, G. K.; Donate, P. M.; Galembeck, S. E. *J. Mol. Struct. (THEOCHEM)* **1997**, *392*, 169.
- Figueiredo, P.; Elhabiri, M.; Saito, N.; Brouillard, R. *Phytochemistry* **1995**, *41*, 301.
- Pereira, G. K.; Donate, P. M.; Galembeck, S. E. *J. Mol. Struct. (THEOCHEM)* **1996**, *363*, 87.
- Mateus, M.; Carvalho, E.; Carvalho, A. R. F.; Melo, A.; González-Paramás, A. M.; Santos-Buelga, C.; Silva, A. M. S.; de Freitas, V. *J. Agric. Food Chem.* **2003**, *51*, 277.
- Meyer, M. *Int. J. Quantum Chem.* **2000**, *76*, 724.
- Woodford, J. N. *Chem. Phys. Lett.* **2005**, *410*, 182.
- Sakata, K.; Saito, N.; Honda, T. *Tetrahedron* **2006**, *62*, 3721.
- Miertu, S.; Scrocco, E.; Tomasi, J. *Chem. Phys.* **1981**, *55*, 117.
- Cossi, M.; Barone, V.; Cammi, R.; Tomasi, J. *Chem. Phys. Lett.* **1996**, *255*, 327.
- (a) Becke, A. D. *J. Chem. Phys.* **1993**, *98*, 5648. (b) Lee, C.; Yang, G.; Parr, R. G. *Phys. Rev.* **1988**, *37*, 785.
- Frisch, M. J.; Trucks, G. W.; Schlegel, H. B.; Scuseria, G. E.; Robb, M. A.; Cheeseman, J. R.; Montgomery, J. A., Jr.; Vreven, T.; Kudin, K. N.; Burant, J. C.; Millam, J. M.; Iyengar, S. S.; Tomasi, J.; Barone, V.; Mennucci, B.; Cossi, M.; Scalmani, G.; Rega, N.; Petersson, G. A.; Nakatsuji, H.; Hada, M.; Ehara, M.; Toyota, K.; Fukuda, R.; Hasegawa, J.; Ishida, M.; Nakajima, T.; Honda, Y.; Kitao, O.; Nakai, H.; Klene, M.; Li, X.; Knox, J. E.; Hratchian, H. P.; Cross, J. B.; Bakken, V.; Adamo, C.; Jaramillo, J.; Gomperts, R.; Stratmann, R. E.; Yazyev, O.; Austin, A. J.; Cammi, R.; Pomelli, C.; Ochterski, J. W.; Ayala, P. Y.; Morokuma, K.; Voth, G. A.; Salvador, P.; Dannenberg, J. J.; Zakrzewski, V. G.; Dapprich, S.; Daniels, A. D.; Strain, M. C.; Farkas, O.; Malick, D. K.; Rabuck, A. D.; Raghavachari, K.; Foresman, J. B.; Ortiz, J. V.; Cui, Q.; Baboul, A. G.; Clifford, S.; Cioslowski, J.; Stefanov, B. B.; Liu, G.; Liashenko, A.; Piskorz, P.; Komaromi, I.; Martin, R. L.; Fox, D. J.; Keith, T.; Al-Laham, M. A.; Peng, C. Y.; Nanayakkara, A.; Challacombe, M.; Gill, P. M. W.; Johnson, B.; Chen, W.; Wong, M. W.; Gonzalez, C.; Pople, J. A. *Gaussian 03*, Revision C.02; Gaussian, Inc.: Wallingford, CT, 2004.
- Tomasi, J.; Mennucci, B.; Cammi, R. *Chem. Rev.* **2005**, *105*, 2999.
- Bader, R. F. W. *Atoms in Molecules: A Quantum Theory*; Oxford University Press: New York, 1990.
- (a) Klamt, A. *Cosmo-RS: From Quantum Chemistry to Fluid Phase Thermodynamics and Drug Design*; Elsevier: Amsterdam, 2005. (b) Fournier, R.; Cheng, J. B. Y.; Wong, A. J. *Chem. Phys.* **2003**, *119*, 9444.
- Allinger, N. L.; Yuh, Y. H.; Lii, J. H. *J. Am. Chem. Soc.* **1989**, *111*, 8551.

- (34) Rappé, A. K.; Casewit, C. J. *Molecular Mechanics across Chemistry*; University Science Books: Sausalito, CA, 1997.
- (35) Harman, D. *J. Gerontol.* **1956**, *2*, 298.
- (36) Harman, D. *J. Proc. Natl. Acad. Sci. U.S.A.* **1981**, *78*, 7124.
- (37) Ozawa, T. *Physiol. Rev.* **1997**, *77*, 425.
- (38) Beckman, K. B.; Ames, B. N. *Physiol. Rev.* **1998**, *78*, 547.
- (39) Sartor, V.; Henderson, P. T.; Schuster, G. B. *J. Am. Chem. Soc.* **1999**, *121*, 11027.
- (40) Leopoldini, M.; Marino, T.; Russo, N.; Toscano, M. *J. Phys. Chem. A* **2004**, *108*, 4916.
- (41) Mandado, M.; Graña, A. M.; Mosquera, R. A. *Chem. Phys. Lett.* **2004**, *400*, 169.
- (42) Gonzalez-Moa, M. J.; Mandado, M.; Mosquera, R. A. *Chem. Phys. Lett.* **2006**, *424*, 17.
- (43) Lien, E. J.; Ren, S.; Bui, H. H.; Wang, R. *Free Radical Biol. Med.* **1999**, *26*, 285.
- (44) Leopoldini, M.; Pitarch, I. P.; Russo, N.; Toscano, M. *J. Phys. Chem. A* **2004**, *108*, 92.
- (45) Leopoldini, M.; Marino, T.; Russo, N.; Toscano, M. *Theor. Chem. Acc.* **2004**, *111*, 210.
- (46) de Heer, M. I.; Korth, H. G.; Mulder, P. *J. Org. Chem.* **1999**, *64*, 6969.
- (47) Zhang, H. Y.; Ji, H. F. *New J. Chem.* **2006**, *30*, 503.
- (48) Leopoldini, M.; Russo, N.; Toscano, M. *J. Agric. Food Chem.* **2006**, *54*, 3078.
- (49) Russo, N.; Toscano, M.; Uccella, N. *J. Agric. Food Chem.* **2000**, *48*, 3232.
- (50) Martins, H. F. P.; Leal, J. P.; Fernandez, M. T.; Lopes, V. H. C.; Cordeiro, M. N. D. S. *J. Am. Soc. Mass Spectrom.* **2004**, *15*, 848.
- (51) Fernandez, M. T.; Mira, L.; Florêncio, M. H.; Jennings, K. R. *J. Inorg. Biochem.* **2002**, *92*, 105.
- (52) Biegler-König, F. W.; Schönbohm, J.; Bayles, D. *J. Comp. Chem.* **2001**, *22*, 545.